DOI: 10.1002/chem.200903353

A Conjugated Thiophene-Based Rotaxane: Synthesis, Spectroscopy, and Modeling

Leszek Zalewski,*[a] Michael Wykes,[b] Sergio Brovelli,[c] Massimo Bonini,[a]
Thomas Breiner,[a] Marcel Kastler,[a] Florian Dötz,[d] David Beljonne,*[b]
Harry L. Anderson,*[e] Franco Cacialli,*[c] and Paolo Samorì*[f, g]

Abstract: A dithiophene rotaxane **1**$\subset\beta$-CD and its shape-persistent corresponding dumbbell **1** were synthesized and fully characterized. 2D NOESY experiments, supported by molecular dynamics calculations, revealed a very mobile macrocycle (β-CD). Steady-state and time-resolved photoluminescence experiments in solution were employed to elucidate the excited-state dynamics for both systems and to explore the effect of cyclodextrin encapsulation. The photoluminescence (PL) spectrum of **1**$\subset\beta$-CD was found to be blueshifted with respect to the dumbbell **1** (2.81 and 2.78 eV, respectively). Additionally, in contrast to previous observations, neither PL spectra nor the decay kinetics of both threaded and unthreaded systems showed changes upon increasing the concentration or changing the polarity of the solutions, thereby providing evidence for a lack of tendency toward aggregation of the unthreaded backbone.

Keywords: conjugation · oligothiophenes · optoelectronics · rotaxanes · supramolecular chemistry

Introduction

Organic π-conjugated molecules incorporating electron-rich thiophene moieties are an important and widely investigated class of semiconductors.[1] In view of their capability of transporting charges, oligothiophenes are attractive building blocks for organic electronic applications including field-effect transistors (FET),[2] light-emitting diodes (LED),[3] and solar cells.[4]

Achieving a full control over the intermolecular interactions in π-conjugated materials makes it possible to optimize several physicochemical properties of the ensemble including its optical and electronic properties. Among various noncovalent engineering strategies, the encapsulation of conjugated molecules by nonconjugated macrocycles to form rotaxanes was shown to represent a powerful method to achieve a high degree of control over several properties of molecular-based systems, as it can allow for simultaneous 1) improvement of molecular rigidity, 2) prevention of aggregation, 3) enhanced solubility and chemical compatibility, as well as 4) protection of the functional unit. The latter is of importance when working with electron-rich chromophores such as oligothiophenes,[5] since the shielding effect of cyclodextrins can hinder radical or electrophilic attack of

---

[a] Dr. L. Zalewski, Dr. M. Bonini, Dr. T. Breiner, Dr. M. Kastler
BASF SE, 67056 Ludwigshafen (Germany)
E-mail: leszekzalewski@gmail.com

[b] M. Wykes, Dr. D. Beljonne
Laboratory for Chemistry of Novel Materials
Université de Mons, 20, Place du Parc, 7000 Mons (Belgium)
E-mail: david@averell.umh.ac.be

[c] Dr. S. Brovelli, Prof. F. Cacialli
Department of Physics and Astronomy (CMMP Group)
and London Centre for Nanotechnology
University College London, Gower Street, London (UK)
E-mail: f.cacialli@ucl.ac.uk

[d] Dr. F. Dötz
BASF SE, Global Research Center Singapore/Organic Electronics
61 Science Park Road, 117525 (Singapore)

[e] Prof. H. L. Anderson
University of Oxford, Department of Chemistry
Chemistry Research Laboratory
Mansfield Road, Oxford OX1 3TA (UK)
E-mail: harry.anderson@chem.ox.ac.uk

[f] Prof. P. Samorì
Nanochemistry Laboratory, ISIS-CNRS 7006
Université de Strasbourg
8 allée Gaspard Monge, 67000 Strasbourg (France)
E-mail: samorì@isis-ulp.org

[g] Prof. P. Samorì
ISOF-CNR, via Gobetti 101, 40129 Bologna (Italy)

the conjugated backbone. In addition, the electronic properties of noncovalently interlocked chromophores inside the cavity were found to be only mildly affected by the environment.

Insulation of chromophores by cyclodextrin (α, β, or γ) macrocycles can significantly reduce interchain electronic interactions within thin films[6] to limit redshift and quenching of the luminescence.[7–10] Hitherto insulated molecular wires have been formed by threading a relatively rigid polymer backbone (i.e., dumbbell) through various types of rings like cyclophanes,[11] cyclodextrins,[9,12,13] or incorporated into inert matrixes of porous materials (zeolites, silica),[14] or even wrapped by polymers.[15] A wide range of host–guest inclusion complexes of cyclodextrins with organic dyes and chromophores in aqueous solutions have been reported. The formation of the inclusion complex relies on the effect of hydrophobic forces to promote penetration of a cyclic cavity by organic molecules, thus leading to stable complexes.[16] The best environment for such a threading reaction is therefore the aqueous media, thereby rendering Suzuki coupling in water a suitable reaction for synthesizing cyclodextrin-encapsulated rotaxanes. Under these conditions, bulky stoppers are typically covalently attached in the α and ω position of the guest molecules to trap the macrocycle and prevent it from unthreading.[9,17]

Despite the great effort devoted to polymer-based rotaxanes, less attention has been paid to oligomeric (i.e., monodisperse) derivatives. Monodisperse rotaxanes offer greater control over the formation of structurally defined architectures featuring preprogrammed electronic and photonic properties.[18] Additionally, monodispersity of π-conjugated oligomers allows for 2D and 3D crystal engineering. The knowledge gained on oligomeric systems is a first step toward attaining a greater understanding of the properties and behavior of the polymer analogues.

Here we describe the synthesis of a novel π-conjugated 2,2′-bithiophene with bulky *m*-terphenylene stoppers encapsulated by β-cyclodextrin. The structure of the derived [2]rotaxane was confirmed by mass spectrometry, 1D and 2D NMR spectroscopy, and modeling. The photophysical properties of derived molecules in solution were investigated by means of time-correlated single-photon counting technique in solution and quantum-chemical calculations. For the sake of comparison, all the properties of the rotaxane were compared to those of the corresponding dumbbell.

Results and Discussion

Synthesis and solution characterization: In aqueous solutions, oligothiophenes form strong and stable complexes with native β-cyclodextrin and its derivatives (such as hydroxypropyl-β-cyclodextrin and dimethyl-β-cyclodextrin).[19] Thiophene-based polypseudorotaxanes were readily synthesized by electropolymerization and chemical oxidation of 2,2′-bithiophenes with $FeCl_3$.[20] The first polythiophene-derived polyrotaxane, with anthracene stoppers, was synthesized by means of a nickel-catalyzed Yamamoto coupling.[21] Both these approaches suffered from a poor control over the polymerization ratio, thus leading to highly polydisperse systems. Additionally, only a maximum 60% of insulation-threading ratio (i.e., 0.6β-cyclodextrin per bithiophene unit) was affordable.

Novel types of oligothiophene rotaxanes were synthesized by Harada and co-workers.[22] By applying aqueous Suzuki coupling conditions, a series of dimethyl-β-cyclodextrin-based rotaxanes that featured various threading ratios and lengths of the conjugated backbone were synthesized by using insulated β-cyclodextrin bulky stoppers.

Instead we opted to focus on ultrarigid oligomeric thiophene-phenyl-based scaffolds as backbone, thereby exposing aromatic end groups terminated with carboxylic acid moieties. Thus this class of oligorotaxane combines features that are relevant for both electronic function of the molecule and preprogrammed self-assembly through the interaction between distinct functional groups, namely hydrogen bonding among COOH moieties that belong to adjacent molecules.

Scheme 1 portrays the synthesis of dithiophene rotaxane **1**$\subset$β-CD. Inclusion complex **3** was formed in a threading reaction between dithiophene diboronic ester **2** and a fourfold molar excess of β-cyclodextrin (β-CD). In the final stage, complex **3** was capped by bulky iodoterphenylenedicarboxylic acid **4** by means of an aqueous Suzuki coupling to yield the formation of a rotaxane. Dithiophene rotaxane **1**$\subset$β-CD was isolated and purified by reversed-phase chromatography (RPC) in 2% yield. Monomer **2** (5,5′-di(1,3,2-dioxaborolan-2-yl)-2,2′-bithiophene) and *m*-terphenylene acid **4** capping group (3,5-bis(4-carboxyphenyl)-1-iodobenzene) were synthesized according to previously reported procedures.[13,22,23]

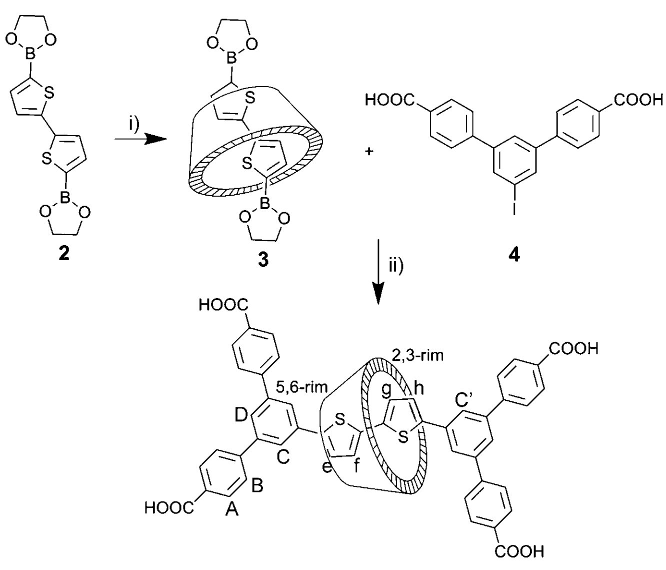

Scheme 1. Synthesis of dithiophene rotaxane **1**$\subset$β-CD. Reagents and conditions: i) water, β-cyclodextrin, room temperature, 4 h, ii) water, lithium carbonate, palladium(II) acetate, 80 °C, 16 h. Dumbbell **1** was synthesized in a separate reaction under the same conditions, except without the cyclodextrin.

Dumbbell **1** was synthesized in a separate reaction under the same coupling conditions and purified by reversed-phase chromatography with a 73 % yield.

The chemical structure of the dithiophene rotaxane was confirmed by ESI mass spectrometry and 2D NMR spectroscopy. Figure 1 shows part of the ^{1}H NMR spectra of the dumbbell **1** (Figure 1a) and the rotaxane **1**⊂β-CD (Figure 1b). Dithiophene protons of dumbbell **1** exhibit a simple pattern (two doublets at $\delta = 7.52$ (**f**+**g**) and 7.88 ppm (**e**+**f**)), thus reflecting the symmetric structure. The presence and the influence of the asymmetric β-cyclodextrin in the NMR spectrum of the rotaxane **1**⊂β-CD in Figure 1b are evidenced by the splitting and shifting of dithiophene doublets. Furthermore, an upfield shift of two aromatic protons (**C**) is observed. The proximity of the macrocycle to the dithiophene unit in **1**⊂β-CD was examined by a 2D NOESY experiment (Figure 2). The pattern of NOEs revealed strong through-space contacts between H5 and H6 of the narrow 5,6-rim of β-cyclodextrin with aromatic hydrogen atoms (labeled **C**) of the stopper, whereas hydrogen atom H3 of the wide 2,3-rim showed intense NOEs with two aromatic protons (**C′**). Dithiophene hydrogen atoms of **1**⊂β-CD (labeled **e** and **f**) showed intense interactions with H6 of the narrow 5,6-rim of β-cyclodextrin, whereas hydrogen atoms **h** and **g** exhibited intense NOEs with H3 of the wide rim of the macrocycle. Slightly less intense NOEs are also observed between **f** and H3, **g** and H5, and **C′** and narrow 5,6-rim protons H5, H6, and H6′. To gain information on the position of β-CD with respect to dumbbell **1**, one must consider that the total intensity for a given NOE interaction is a result of an ensemble average over all possible interproton distances. The contribution to the total NOE intensity at each possible interproton distance is the product of the intensity of the NOE interaction (proportional to the inverse sixth power of the interproton distance) and a Boltzmann weight (the value of the probability distribution function (PDF) at that distance). In addition, if multiple protons have the same chemical shift as the equivalent protons in the seven units of β-CD, the intensities for all protons will be summed. Molecular dynamics simulations were employed to gain insight into this complex picture by elucidating the average relative NOE intensity as a function of β-CD position and predicting the PDF. Conclusions concerning the interpretation of the NOESY spectrum and the position of β-CD with respect to dumbbell **1** are presented in the molecular dynamics section below.

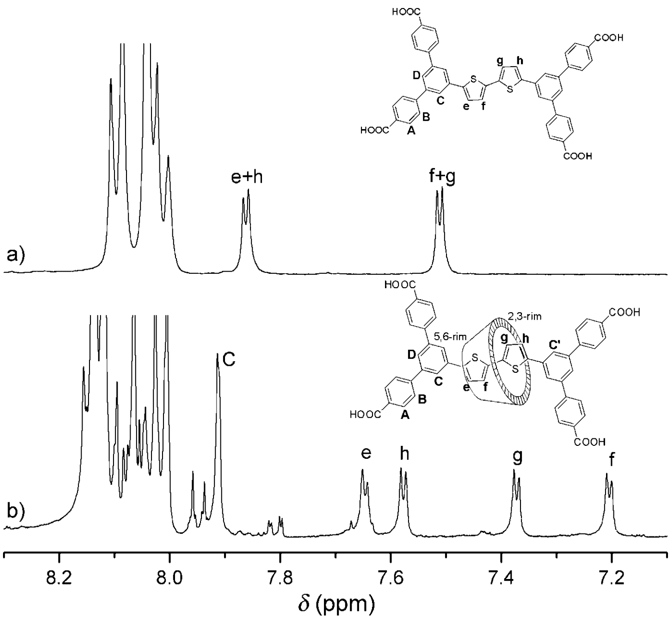

Figure 1. ^{1}H NMR of a) dumbbell **1** and b) rotaxane **1**⊂β-CD in [D$_6$]DMSO at room temperature, 400 MHz. Please note that C′ protons are lying in the range $\delta = 8.0$ and 8.2 ppm.

Molecular dynamics simulations: Computational studies can assist the interpretation of both optical and NMR spectra by elucidating the relationship between structure and spectroscopic response. The combination of molecular modeling and spectroscopies in the characterization of cyclodextrin host–guest complexes has been reviewed by Lipkowitz.[24]

Here we used molecular dynamics (MD) simulations to sample the distribution of β-CD positions and orientations with respect to the dumbbell **1** guest at 300 K. We then calculated relative NOE intensities of proton–proton interac-

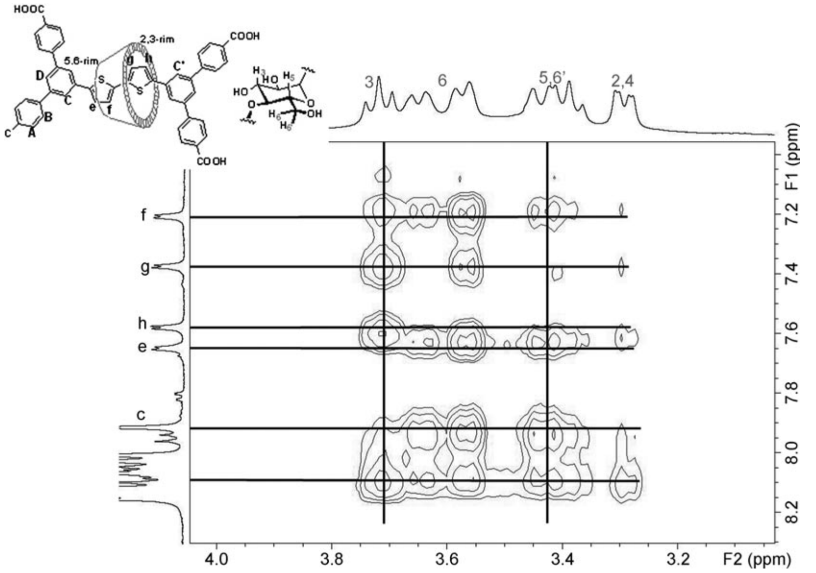

Figure 2. Part of the ^{1}H NMR NOESY spectrum of [2]rotaxane **1**⊂β-CD in [D$_6$]DMSO, at room temperature, 400 MHz. Please note that C′ protons are lying in the range $\delta = 8.0$ and 8.2 ppm.

tions based on the MD trajectory and generated plots of NOE intensity as a function of β-CD position with respect to dumbbell **1**, thereby providing insight into which structures contribute strongly to each peak in the NOESY spectrum. Details of the MD simulations can be found in the Experimental Section.

In quantifying the position of the β-CD along the dithiophene axis, a metric *d* was defined as the distance between the center of mass (COM) of β-CD and the COM of the first benzene ring of the stopper on the wide-rimmed side of the β-CD. The average distance between the first benzene ring of the stopper on the wide-rimmed side of the β-CD and the first benzene ring of the stopper on the narrow-rimmed side of the β-CD amounts to 1.2 nm, so *d* may lie in the range 0 to 1.2 nm with a distance of 0.6 that corresponds to β-CD being perfectly centered along the dithiophene backbone. The metric *d* was measured every 1 ps over a total sampling time of 1.05 μs. If the MD sampling is statistically converged, then a normalized histogram of *d* values will represent the real probability distribution function (PDF), and a potential of mean force (PMF) or the free energy as a function of *d* can be obtained by Boltzmann inversion. Details of how statistical uncertainties were estimated can be found in the Experimental Section. The PDF and PMF of *d* (Figure 3) feature relatively small undulations on the order of KT at 300 K over the range 0.2 to 0.9 nm, indicating that at 300 K BCD can diffuse over this range of the reaction coordinate without encountering significant free energy barriers.

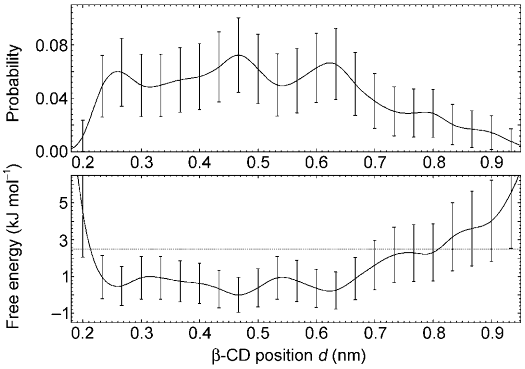

Figure 3. Probability distribution function (PDF) and potential of mean force (PMF) as a function of β-CD position *d*, thus indicating that the macrocycle is very mobile at 300 K. Points are joined by cubic spline interpolations.

To asses the tilt of the β-CD with respect to the dithiophene axis, a second metric θ was defined as the average angle between the dumbbell **1** backbone axis (defined by the backbone terminal carbon atoms) and four vectors that cross the average plane of the β-CD from opposite oxygen linkers (see Figure 4).

The metrics *d* and θ were combined into a two-dimensional histogram shown in Figure 5. This indicates the β-CD can be strongly tilted and that the main probability peak is located at (d,θ) values of (0.47,75), which corresponds to the macrocycle being slightly off center along the dithiophene backbone and slightly tilted (see inset of Figure 4). Smaller peaks and significant nonzero probability over the range $0.2 < d < 0.9$ and $60^\circ < \theta < 90^\circ$ indicate that the free-energy barriers for β-CD to leave the largest probability peak are small and hence that the macrocycle is very mobile at 300 K.

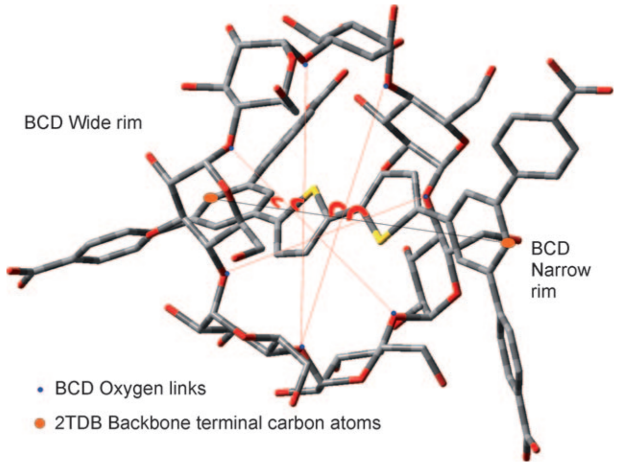

Figure 4. β-CD tilt angle θ defined as the average angle between vectors that connect opposite oxygen linkers and the dumbbell **1** axis vector between backbone terminal carbon atoms. As β-CD contains seven oxygen linkers, the average is over four angles, one of the oxygen atoms being used twice. An angle of 90° corresponds to zero tilt ($\theta = 0^\circ$). Hydrogen atoms have been omitted for clarity.

To check for consistency between the MD results and the NOESY spectrum (Figure 2), we investigated the relationship between intensities of individual NOE peaks and the geometry of the system. NOE intensity of a single-proton pair varies with the inverse sixth power of the distance between the protons. The intensity of protons with identical chemical shifts are summed in the experimental spectrum, so here we sum the inverse sixth powers of interproton distances between all equivalent proton pairs for each frame in the MD trajectory. The dependence of the relative NOE intensity on β-CD position *d* was investigated by binning trajectory frames according to *d* and calculating the average intensity in each histogram bin. The total intensity observed in the spectrum is an ensemble average integral over all possible geometries of the system, which, for the sake of this analysis, we represent as an integral over all *d* of the product of $I(d)$, the average relative NOE intensity as a function of *d* and PDF(d), the probability as a function of *d*. How much information can be gleaned from the integrated total intensity and $I(d)$ depends on how sensitive $I(d)$ is to a change in *d*; if the intensity is constant over all *d* we can learn nothing about the PD; conversely, if the intensity is strong over only a small range of *d*, a weak or strong experimental intensity tells us that the PDF for that *d* range are small or large, respectively. Figure 6 presents a selection of the most intense and *d*-dependent NOE interactions.

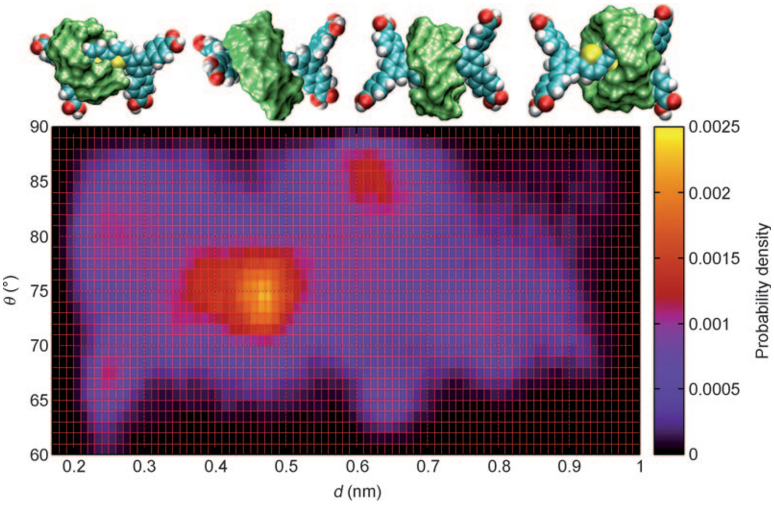

Figure 5. Histogram of β-CD orientation and position and structures from each probability peak. The bin spacing is 0.1 nm for *d* and 1° for the tilt angle *θ*. From left to right the structures shown above have (*d*,*θ*) values of (0.24,67), (0.46,73), (0.6,85), and (0.79,72), respectively. Atoms in the dithiophene dumbbell are represented as van der Waals spheres, whereas the β-CD is represented by bonds and van der Waals surface mesh.

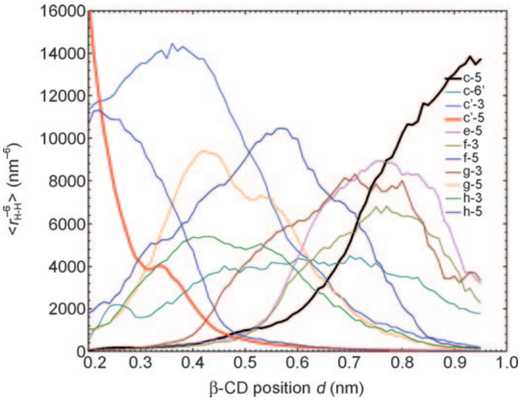

Figure 6. Average proton–proton distances to the inverse sixth power estimating relative NOE intensities as a function of β-CD position. The NOE interactions C′-5 and C-5 are the most sensitive to β-CD position and have been plotted with a thicker line.

Many of the interactions are strong over a wide range of *d*, thus making it impossible to extract information on the β-CD position from the NOESY spectrum with a useful level of resolution. The NOE interactions of **e** and **h** are problematic as they are not particularly well resolved in the spectrum, thereby making it hard to evaluate the total intensity of each interaction separately. **C**′-5 and **C**-5 interactions are, however, sensitive to *d*, the former being intense over the range $d<0.5$, the latter being intense over the range $d>0.5$. Since both interactions feature intense peaks in the spectrum, we can conclude that both regions $d>0.5$ and $d<0.5$ are sampled at 300 K, in agreement with PDF predicted by molecular dynamics simulations.

Our MD simulations also provide information on the timescale of β-CD motion along the dumbbell backbone. The mean-squared displacement of β-CD position *d* as a function of time (not shown) displayed linear behavior between 0.5 and 1 ns. Inserting the slope into the 1D diffusion equation $<|d(t)-d(t_0)|^2>=2Dt$ yielded the diffusion coefficient. Performing this analysis on twenty-one independent MD trajectories yielded an average D of $(4.1\pm1.8)\times10^{-6}$ nm^{2}ps. Using the expression $t=d^2/2D$, the diffusion model predicts that β-CD requires (44±20) ns to diffuse along the backbone from $d=0.25$ to 0.85 nm.

The effect of β-CD on the torsional degrees of freedom of dumbbell **1** was also assessed by comparing the distributions of rotaxinated and nonrotaxinated backbones. Angles for the rotaxinated system were measured over the 1.05 μs trajectory of the solvated system previously described. Angles for the nonrotaxinated system were taken from a 0.6 μs simulation in the gas phase using a stochastic dynamics integrator to mimic the random forces a solvated molecule would be subject to. The distributions were symmetrized by folding thiophene–thiophene (TT) and thiophene–phenyl (TP) torsion angles $-180°<\omega<180°$ into the range $0°<\omega<180°$ and $0°<\omega<90°$, respectively. To quantify the average torsion angle ($<\omega_{90}>$) with respect to planarity, whether *cis* or *trans*, the TT distribution was also folded into the range $0°<\omega<90°$. Figure 7 shows the distribution of TT and TP torsion angles and corresponding $<\omega_{90}>$ values inset. Both distributions indicate a subtle planarization of the dumbbell **1** upon β-CD rotaxination. The average reduction in $<\omega_{90}>$ is 6.3, 4.6, and 1.2° for TP at β-CD narrow rim, TP at β-CD wide rim, and TT, respectively.

Optical properties: We focused our attention on the optical properties of dumbbell **1** and **1**⊂β-CD rotaxane with a view to unravel the kinetics of excited states and their dependence on cyclodextrin encapsulation. Recently, comparison of threaded and unthreaded polymeric systems has allowed significant insight into the consequences of threading on the optical properties of conjugated polymers and on the formation and decay of interchain and intrachain excitonic species.[7,25] With this in mind, we performed steady-state and time-resolved photoluminescence experiments on diluted solutions of **1** and **1**⊂β-CD in dimethyl sulfoxide (DMSO). Both systems are easily soluble in DMSO due to the polarity of the carboxylic units of the bulky end groups.

We started our analysis by considering the optical absorption and time-integrated PL spectra of solutions of **1**⊂β-CD and dumbbell **1** (5×10^{-2} mg mL^{-1} of the conjugated portion) in DMSO, reported in Figure 8. The absorption spectra

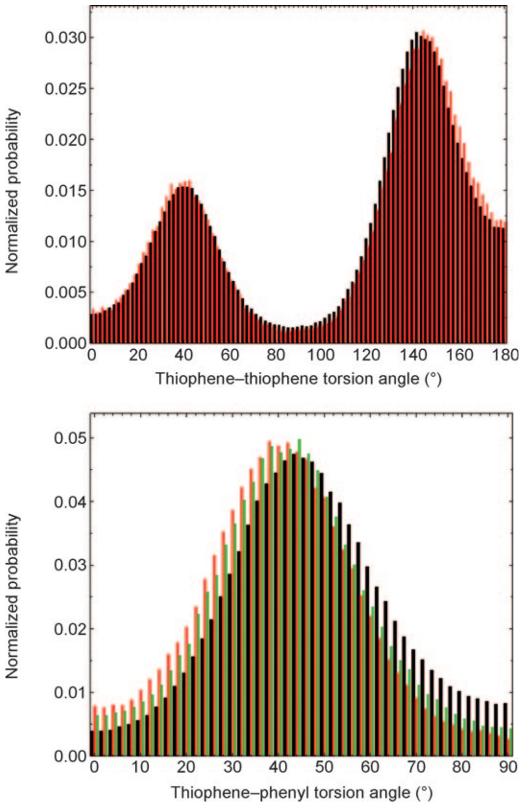

Figure 7. Torsion angle distributions from simulations at 300 K, thus indicating a subtle planarization of the backbone. The value $<\omega_{90}>$ defines the average angle with respect to planarity, whether *cis* or *trans*. a) Black: dumbbell, $<\omega_{90}>=37.13$; red: rotaxane, $<\omega_{90}>=35.92$. b) Black: dumbbell, $<\omega_{90}>=46.84$; red: β-CD narrow rim, $<\omega_{90}>=40.50$; green: β-CD wide rim, $<\omega_{90}>=42.22.7$

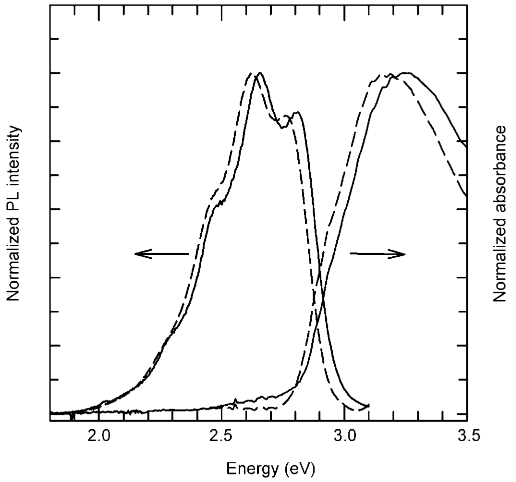

Figure 8. Optical absorption and continuous wave (cw) photoluminescence spectra excited at 3.34 eV for solutions (5×10^{-2} mg mL^{-1} of the conjugated portion) of **1**⊂β-CD and dumbbell **1** in DMSO (——: with β-CD, -----: without β-CD).

show a first absorption band in the UV spectral region at 3.24 and 3.16 eV for the rotaxane and the dumbbell, respectively. The PL spectra of both threaded and unthreaded molecules present a well-defined vibronic structure with a 0–0 fluorescence band at 2.81 and 2.78 eV, respectively. As observed for other encapsulated systems,[8,26] also in this case the PL spectrum of the rotaxane is blueshifted with respect to the unthreaded backbone. Possible causes of this blueshift include a reduction of intermolecular interactions, the modified solvation environment or a sterically driven increase in twist angle between adjacent thiophene units on the backbone. MD simulations indicate, however, that a sterically driven decrease in twist angle between adjacent thiophene units occurs, thereby dismissing the latter potential explanation of the observed blueshift.

To gain further insight into the fluorescence kinetics of the investigated systems, in Figure 9 we report the PL decay curves for both systems collected at the emission maximum in DMSO. The fluorescence kinetics of both threaded and unthreaded systems are single exponential with a lifetime $\tau=505$ ps. This result is consistent with the observation of a similar PL quantum yield for the two systems ($\Phi_{PL}=0.12\pm0.01$) and confirms that the radiative lifetime of intrinsic excitons, $\tau_{RAD}=\tau/\Phi_{PL}=4.2$ ns, is independent of rotaxination.[26] Furthermore, both the spectral properties and decay dynamics suggest that aggregation is strongly disfavored in both investigated systems, possibly as a result of the presence of the carboxylic functionalities on the end groups, the twofold biphenyl twist on each *meta*-terphenyl terminus, and the relatively short length of the dithiophene backbone.

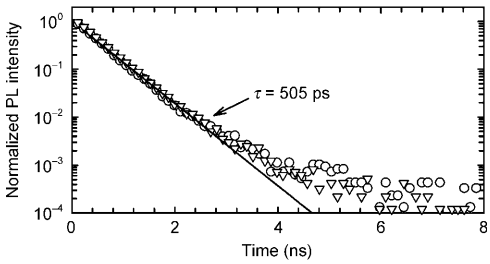

Figure 9. Time-dependent decays of **1**⊂β-CD (circles) and dumbbell **1** (triangles) in DMSO (5×10^{-2} mg mL^{-1}) excited at 3.3 eV. The PL decays were fitted with a single exponential function, thereby yielding an experimental lifetime $\tau=505$ ps. The fitting curve is reported as solid lines (○: with β-CD, ▽: without β-CD).

Excited-state calculations: Finally, we performed excited-state calculations on the series of molecules from bithiophene (2T) to quaterthiophene (4T) as well as the dumbbell **1** to confirm the experimental observation that dumbbell **1** emits at the same energy as 4T, thus indicating that conjugation extends over the first ring of each stopper. Calculations were performed with TURBOMOLE 5.9[27] using time-dependent density functional theory (TD-DFT), the B3LYP functional, the 6-31g(d,p) basis set, the m4 numerical quadrature grid, and an SCF convergence criterion of 10^{-7}. The geometry of the lowest singlet electronic excited state of each molecule was optimized in the gas phase, thereby yielding emission vertical transition energies. Vertical transition (VT) energies can also be extracted from the experimental fluorescence spectra by calculating the intensity-weighted average transition energy. Values for thiophene oligomers were based on fluorescence spectra from ref. [23]. Figure 10 plots the predicted VT energy versus the experimental one. This confirms that dumbbell **1** does indeed emit at very similar energies to 4T. Differences between the experimental and predicted energies are likely due to the limitations of the B3LYP functional and also the lack of a treatment of solvent effects.

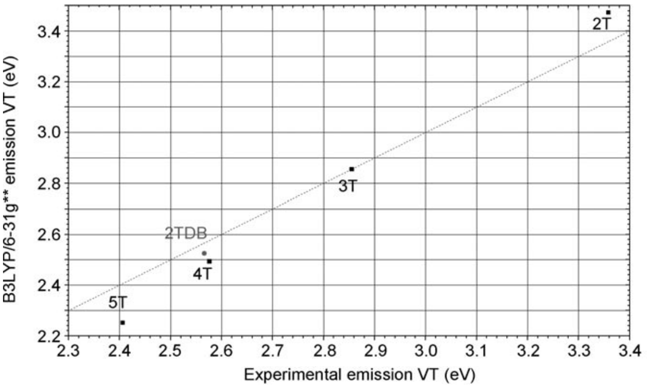

Figure 10. Predicted- and measured-emission vertical-transition energies that indicate that dumbbell **1** emits at similar energies to 4T and hence that conjugation extends over the first ring of each stopper (■: thiophene series, ●: dumbbell).

Conclusion

In summary, we have described a joint synthetic, analytical, optical, and computational investigation of a new rigid dithiophene β-CD rotaxane and its related dumbbell.

In DMSO, the presence of the threaded cyclodextrin has only a subtle effect on the absorption and emission behavior of the π system.

Molecular dynamics simulations provided direct evidence for the spatial distribution and orientation of β-CDs with respect to the dumbbell, whereas excited-state calculations supported the optically detected extended conjugation for both investigated molecules.

It was shown that β-CD is slightly tilted and centered along the dithiophene backbone, with mobile ability over the range 0.2 to 0.9 nm at 300 K. Due to reduced intermolecular interaction, blueshifted absorption and photoluminescence were observed. Our dithiophene β-CD rotaxane, being based on a conformationally rigid and conjugated backbone, represents a model system to explore the optoelectronic properties of insulated molecular wires.

Experimental Section

Diboronic ester **2** (5,5′-di(1,3,2-dioxaborolan-2-yl)-2,2′-bithiophene)[22] and aryl iodide stopper **4** (3,5-bis(4-carboxyphenyl)iodobenzene) were synthesized according to previously reported procedures.[23]

Experimental procedures: ^{1}H NMR spectra were recorded using a Bruker Avance 400 spectrometer at 400 MHz. The residual solvent peak was used as reference for calibration ([D$_6$]DMSO: $\delta = 2.50$ ppm). Peaks are described as singlet (s), doublet (d), triplet (t), doublet of doublet (dd), and multiplet (m). Unless otherwise noted, spectra were recorded at 25 °C. ^{13}C NMR spectra were recorded using a Bruker Advance 400 spectrometer at 100 MHz. All spectra were measured in broadband decoupled conditions. Chemical shifts are given in ppm. The residual solvent peak was taken as reference ([D$_6$]DMSO: $\delta = 39.43$ ppm). Unless otherwise noted, spectra were recorded at 25 °C. 2D NMR (COSY, NOESY) were recorded using a Bruker Avance 400 spectrometer. High-resolution mass spectrometry (HRMS) analyses were performed using a Bruker Micro TOF mass spectrometer at the Service de Spectrométrie de Masse, Université de Strasbourg. The observed pattern was always compared to the theoretical pattern.

Synthesis of dumbbell 1: A solution of diboronic ester **2** (0.020 mmol, 6.8 mg), aryl iodide stopper **4** (0.045 mmol, 20 mg), lithium carbonate (0.18 mmol, 13 mg), and palladium(II) acetate (4.5 μmol, 1.0 mg) in water (degassed and nitrogen saturated, 5.0 mL) was heated to 80 °C for 18 h, then allowed to cool. Hydrochloric acid (2.0 M) was added to give a gelatinous precipitate that was collected by centrifugation and washed with water (2 × 15 mL). The crude product was redissolved in DMSO, filtered, and concentrated to 4 mL. Methanol was added to form a greenish precipitate, which was collected by using a centrifuge. The crude product was purified on RP silica (gradient: H_2O to H_2O/CH_3CN 20 %) to give a greenish solid (13 mg). Yield: 73 %. ^{1}H NMR (400 MHz, DMSO, RT): $\delta = 7.52$ (d, $J = 3.6$ Hz, 2 H), 7.88 (d, $J = 3.6$ Hz, 2 H), 8.03 (m, 14 H), 8.09 ppm (m, 8 H); ^{13}C NMR (100 MHz, DMSO, RT): $\delta = 93.81$, 123.97, 127.81, 130.39, 130.56, 135.28, 136.70, 141.32, 142.05, 144.00, 167.54 ppm; MS (ESI): m/z: calcd for $C_{48}H_{29}O_8S_2$: 797.13 $[M-H]^-$; found: 797.09.

Synthesis of [2]rotaxane 1⊂β-CD: A solution of diboronic ester **2** (0.30 mmol, 96 mg) and β-cyclodextrin (1.2 mmol, 1.4 g) in water (8.0 mL, degassed and nitrogen saturated) was stirred for 4 h at room temperature, and then added to the reaction mixture containing aryl iodide stopper **4** (0.60 mmol, 280 mg), lithium carbonate (2.4 mmol, 180 mg), and palladium(II) acetate (36 μmol, 8 mg) in water (degassed and nitrogen saturated, 60 mL). The reaction mixture was heated to 80 °C overnight under nitrogen, then allowed to cool. Hydrochloric acid (2 M) was added to give a gelatinous precipitate that was collected by centrifugation and washed with water (6 × 15 mL). Collected precipitate was dissolved in DMSO, filtered, and concentrated to 12 mL; chloroform was added to form a precipitate that was collected by using a centrifuge. Crude product (containing dumbbell and [2]rotaxane) was dissolved in Li_2CO_3 solution (90 mmol) and purified on RP silica column (gradient: H_2O to H_2O/CH_3CN 10 %), thereby eluting [2]rotaxane and dumbbell. Both fractions were concentrated to a volume of 5 mL and acidified by 0.5 M HCl to give precipitates that were collected by using a centrifuge, washed with water, and dried. Yield: 2 % of [2]rotaxane **1⊂β-CD** (12 mg, yellowish solid) and 62 % of dumbbell **1** (148 mg, greenish solid). For [2]rotaxane (**1⊂β-CD**): ^{1}H NMR (400 MHz, DMSO, RT): $\delta = 3.29$ (m, 7 H), 3.41 (m, 21 H), 3.57 (d, $J = 9.6$ Hz, 7 H), 3.65 (d, $J = 9.2$ Hz, 7 H), 3.71 (t, $J = 9.2$ Hz, 7 H), 4.80 (d, $J = 3.2$ Hz, 7 H), 7.20 (d, $J = 3.6$ Hz, 1 H), 7.36 (d, $J = 3.6$ Hz, 1 H), 7.57 (d, $J = 3.6$ Hz, 1 H), 7.64 (d, $J = 3.6$ Hz, 1 H), 7.91 (s, 2 H), 8.00 (s, 2 H), 8.02 (s, 2 H), 8.06 (s, 4 H), 8.09 (m, 2 H), 8.13 ppm (m, 10 H); ^{13}C NMR (100 MHz, DMSO, RT): $\delta = 60.04$, 72.40, 72.83, 73.51, 81.77, 102.42, 124.80, 127.70, 127.99, 130.56, 141.13, 141.44, 142.76, 144.03, 167.63, 167.77 ppm; MS (ESI): m/z: calcd for $C_{90}H_{100}O_{43}S_2$: 1931.49 $[M-H]^-$; found: 1931.41.

Molecular modeling: In our MD simulations, **1** was modeled using a modified version of the OPLSAA[28] forcefield (FF). Modifications included deriving partial atomic charges fitted to the B3LYP/6-31g(d,p)//MP2/6-31g(d,p) electrostatic potential using restraints[29] to ensure equal charges on equivalent atoms. The forcefield was also modified to reproduce the accurate MP2/aug-cc-VTZ potentials of bithiophene,[30] biphenyl,[31] and thiophene phenyl (performed ourselves at the MP2/6-31g(d,p)//MP2/aug-cc-VTZ level using Gaussian 03[32]). β-CD was modeled using the OPLSAA forcefield for carbohydrates,[33] whereas the solvent DMSO was modeled using the united atom OPLS forcefield.[34]

MD simulations were performed on a system that comprised the **1**⊂β-CD rotaxane solvated in a cubic box of 422 DMSO molecules using GROMACS 4.05.[35] The system was simulated in the NPT ensemble, the temperature being regulated using the Nose–Hoover algorithm (300 K, 0.1 ps coupling time) and the pressure regulated using the Berendsen algorithm (1 atm, 1 ps coupling time). During the simulations, the equations of motion were integrated using a time step of 2 fs and all bond lengths were fixed at their equilibrium values. Nonbonded interactions were calculated up to a cut-off distance of 1.5 nm. After an initial equilibration period, the β-CD was pulled from one end of the **1** to the other by applying harmonic restraints to the distance (d) between the β-CD center of mass (COM) and the COM of the first phenyl of the stopper on the wide-rimmed side of the β-CD over a period of 10 ns. Twenty-one geometries evenly spaced along the range of $d = 0.05$–1.15 nm were taken from the restrained trajectory and given new random velocities. Each was then simulated for 50 ns without restraints, thereby resulting in a total of 1.05 μs sampling time.

Assuming fully converged MD sampling, it is possible to determine the PMF along d by Boltzmann-inverting the probability distribution. If the sampling is not fully converged, there will be statistical uncertainties in the probability distribution and corresponding uncertainties in the derived PMF. High energy-barrier regions are sampled less frequently than lower-lying regions and thus suffer the largest statistical uncertainties and introduce the largest errors into the PMF. These statistical uncertainties can be estimated by bootstrapping,[36] and here we perform the analysis as implemented in the WHAM code.[37] The correlation time after which points in the time series were assumed to be uncorrelated in the bootstrapping analysis was estimated by means of block averaging (see ref. [38] for a review) to be 12 ns. Data points in the range 0.15 to 1.15 nm were binned into 30 bins to yield the histogram approximation to the PDF. Binning the same data into 110 bins resulted in a near-identical PMF after Boltzmann inversion, thus indicating that the binning with 30 bins was not artificially smoothing the PMF. Due to the flatness of the PMF over the range $d = 0.2$ to 0.9 nm, this region is well sampled and the statistical uncertainties in the probability and free energies are acceptably small (see Figure 3).

Optical characterization: All data shown were taken for 5×10^{-2} mg mL^{-1} solutions of dumbbell **1** and **1**⊂β-CD [2]rotaxane in DMSO. The solutions were investigated in a Spectrosil fluorescence cuvette. Their concentrations were determined by measuring their optical absorption spectra in the visible and near-ultraviolet (UV) region by means of a CCD-based spectrophotometer (Agilent 8543) with a spectral resolution of 1 nm. Decay dynamics were studied with a time-correlated single-photon counting (TCSPC) setup (Edinburgh Instruments) that consisted of a ps-pulsed diode laser at 375 nm (Edinburgh Instruments EPL-375) and a F-900 TCSPC unit (temporal resolution ≈150 ps) with a photomultiplier tube coupled to a monochromator. The photoluminescence quantum yields (Φ) have been measured using a relative method for optical dilute solutions, using as reference the quantum yield of quinine sulfate dehydrate in 1.0 N sulfuric acid ($\approx10^{-5}$ M; $\Phi = (0.546\pm5)$ %; NIST standard reference material SRM# 936a).[39] The aggregation properties of **1**⊂β-CD and dumbbell **1** were investigated by measuring their PL spectra and decay curves in DMSO either at increasing molecular concentration (from 1 mg mL^{-1} to 5×10^{-2} mg mL^{-1} of the conjugated portion) or by titrating the solutions with dichloromethane (from 10 to 99 % in volume) using the same diode laser and TCSPC unit described above. All experiments were performed at room temperature and all measurements were corrected for the overall spectral response.

Acknowledgements

Alan Grossfield is acknowledged for helpful discussions concerning the statistical uncertainties in the PMF. This work was supported by the EC Marie Curie projects THREADMILL (MRTN-CT-2006-036040) and SUPERIOR (PITN-CT-2009-238177), the EC FP7 ONE-P large-scale project no. 212311, the NanoSci-E+ project SENSORS, the ESF-SONS2-SUPRAMATES project, and the International Center for Frontier Research in Chemistry (FRC). The work in Mons is partly supported by the Interuniversity Attraction Pole IAP 6/27 of the Belgian Federal Governement, and the Belgian National Fund for Scientific Research (FNRS/FRFC). The calculations were carried out at the Interuniversity Scientific Calculation Facility (FUNDP, Namur, Belgium), for which the authors gratefully acknowledge the financial support of FNRS-FRFC. D.B. is a FNRS Research Director.

---

[1] D. Fichou, *Handbook of Oligo-and Polythiophenes*, Wiley-VCH Weinheim, **1999**; I. F. Perepichka, D. F. Perepichka, *Handbook of Thiophene-Based Materials 2 V Set: Applications in Organic Electronics and Photonics*, Wiley-Blackwell, New York, **2009**; A. P. H. J. Schenning, A. F. M. Kilbinger, F. Biscarini, M. Cavallini, H. J. Cooper, P. J. Derrick, W. J. Feast, R. Lazzaroni, P. Leclere, L. A. McDonell, E. W. Meijer, S. C. J. Meskers, *J. Am. Chem. Soc.* **2002**, *124*, 1269; F. Biscarini, R. Zamboni, P. Samorì, P. Ostoja, C. Taliani, *Phys. Rev. B* **1995**, *52*, 14868; P. Leclère, M. Surin, P. Viville, R. Lazzaroni, A. F. M. Kilbinger, O. Henze, W. J. Feast, M. Cavallini, F. Biscarini, A. P. H. J. Schenning, E. W. Meijer, *Chem. Mater.* **2004**, *16*, 4452.

[2] X. M. Hong, H. E. Katz, A. J. Lovinger, B.-C. Wang, K. Raghavachari, *Chem. Mater.* **2001**, *13*, 4686; M. Mushrush, A. Facchetti, M. Lefenfeld, H. E. Katz, T. J. Marks, *J. Am. Chem. Soc.* **2003**, *125*, 9414; F. Dinelli, M. Murgia, P. Levy, M. Cavallini, F. Biscarini, D. M. de Leeuw, *Phys. Rev. Lett.* **2004**, *92*.

[3] A. Kraft, A. C. Grimsdale, A. B. Holmes, *Angew. Chem.* **1998**, *110*, 416; *Angew. Chem. Int. Ed.* **1998**, *37*, 402; A. G. MacDiarmid, *Angew. Chem.* **2001**, *113*, 2649; *Angew. Chem. Int. Ed.* **2001**, *40*, 2581.

[4] Y. Kim, S. Cook, S. M. Tuladhar, S. A. Choulis, J. Nelson, J. R. Durrant, D. D. C. Bradley, M. Giles, I. McCulloch, C.-S. Ha, M. Ree, *Nat. Mater.* **2006**, *5*, 197; X. Yang, J. Loos, S. C. Veenstra, W. J. H. Verhees, M. M. Wienk, J. M. Kroon, M. A. J. Michels, R. A. J. Janssen, *Nano Lett.* **2005**, *5*, 579.

[5] A. Facchetti, *Mater. Today* **2007**, *10*, 28; E. Arunkumar, N. Fu, B. D. Smith, *Chem. Eur. J.* **2006**, *12*, 4684.

[6] J. S. Wilson, M. J. Frampton, J. J. Michels, L. Sardone, G. Marletta, R. H. Friend, P. Samorì, H. L. Anderson, F. Cacialli, *Adv. Mater.* **2005**, *17*, 2659.

[7] A. Petrozza, S. Brovelli, J. J. Michels, H. L. Anderson, R. H. Friend, C. Silva, F. Cacialli, *Adv. Mater.* **2008**, *20*, 3218.

[8] F. Cacialli, J. S. Wilson, J. J. Michels, C. Daniel, C. Silva, R. H. Friend, N. Severin, P. Samorì, J. P. Rabe, M. J. O'Connell, P. N. Taylor, H. L. Anderson, *Nat. Mater.* **2002**, *1*, 160.

[9] P. N. Taylor, M. J. O'Connell, L. A. McNeill, M. J. Hall, R. T. Aplin, H. L. Anderson, *Angew. Chem.* **2000**, *112*, 3598; *Angew. Chem. Int. Ed.* **2000**, *39*, 3456.

[10] C. Y. Chi, A. Mikhailovsky, G. C. Bazan, *J. Am. Chem. Soc.* **2007**, *129*, 11134; F. E. Oddy, S. Brovelli, M. T. Stone, E. J. F. Klotz, F. Cacialli, H. L. Anderson, *J. Mater. Chem.* **2009**, *19*, 2846.

[11] J. Buey, T. M. Swager, *Angew. Chem.* **2000**, *112*, 622; *Angew. Chem. Int. Ed.* **2000**, *39*, 608; S. Anderson, R. T. Aplin, T. D. W. Claridge, T. G. Iii, A. C. Maciel, G. Rumbles, J. F. Ryan, H. L. Anderson, *J. Chem. Soc. Perkin Trans. 1* **1998**, 2383; J.-P. Sauvage, J.-M. Kern, G. Bidan, B. Divisia-Blohorn, P.-l. Vidal, *New J. Chem.* **2002**, *26*, 1287; T. Ikeda, M. Higuchi, A. Sato, D. G. Kurth, *Org. Lett.* **2008**, *10*, 2215; T. Ikeda, M. Higuchi, D. G. Kurth, *Chem. Eur. J.* **2009**, *15*, 4906.

[12] M. R. Craig, M. G. Hutchings, T. D. W. Claridge, H. L. Anderson, *Angew. Chem.* **2001**, *113*, 1105; *Angew. Chem. Int. Ed.* **2001**, *40*,

1071; S. Anderson, T. D. W. Claridge, H. L. Anderson, *Angew. Chem.* **1997**, *109*, 1367; *Angew. Chem. Int. Ed. Engl.* **1997**, *36*, 1310; H. Onagi, C. J. Blake, C. J. Easton, S. F. Lincoln, *Chem. Eur. J.* **2003**, *9*, 5978; Q.-C. Wang, X. Ma, D.-H. Qu, H. Tian, *Chem. Eur. J.* **2006**, *12*, 1088; S. A. Nepogodiev, J. F. Stoddart, *Chem. Rev.* **1998**, *98*, 1959; R. S. Wylie, D. H. Macartney, *J. Am. Chem. Soc.* **1992**, *114*, 3136; H. Murakami, A. Kawabuchi, K. Kotoo, M. Kunitake, N. Nakashima, *J. Am. Chem. Soc.* **1997**, *119*, 7605; M. R. Craig, T. D. W. Claridge, H. L. Anderson, M. G. Hutchings, *Chem. Commun.* **1999**, 1537; C. A. Stanier, M. J. O'Connell, H. L. Anderson, W. Clegg, *Chem. Commun.* **2001**, 493; J. Terao, A. Tang, J. J. Michels, A. Krivokapic, H. L. Anderson, *Chem. Commun.* **2004**, 56.

[13] J. J. Michels, M. J. O'Connell, P. N. Taylor, J. S. Wilson, F. Cacialli, H. L. Anderson, *Chem. Eur. J.* **2003**, *9*, 6167.

[14] T. Q. Nguyen, J. Wu, S. H. Tolbert, B. J. Schwartz, *Adv. Mater.* **2001**, *13*, 609; D. J. Cardin, *Adv. Mater.* **2002**, *14*, 553; T. Bein, P. Enzel, *Angew. Chem.* **1989**, *101*, 1737; *Angew. Chem. Int. Ed. Engl.* **1989**, *28*, 1692; D. J. Cardin, S. P. Constantine, A. Gilbert, A. K. Lay, M. Alvaro, M. S. Galletero, H. Garcia, F. Marquez, *J. Am. Chem. Soc.* **2001**, *123*, 3141; V. S. Y. Lin, D. R. Radu, M.-K. Han, W. Deng, S. Kuroki, B. H. Shanks, M. Pruski, *J. Am. Chem. Soc.* **2002**, *124*, 9040.

[15] M. J. Frampton, T. D. W. Claridge, G. Latini, S. Brovelli, F. Cacialli, H. L. Anderson, *Chem. Commun.* **2008**, 2797.

[16] K. Harata, *Chem. Rev.* **1998**, *98*, 1803; M. V. Rekharsky, Y. Inoue, *Chem. Rev.* **1998**, *98*, 1875.

[17] M. J. Frampton, H. L. Anderson, *Angew. Chem.* **2007**, *119*, 1046; *Angew. Chem. Int. Ed.* **2007**, *46*, 1028; J. Terao, S. Tsuda, Y. Tanaka, K. Okoshi, T. Fujihara, Y. Tsuji, N. Kambe, *J. Am. Chem. Soc.* **2009**, *131*, 16004.

[18] K. Müllen, G. Wegner, *Electronic Materials: The Oligomer Approach*, Wiley-VCH, Weinheim, **1998**.

[19] C. Lagrost, K. I. C. Ching, J.-C. Lacroix, S. Aeiyach, M. Jouini, P.-C. Lacaze, J. Tanguy, *J. Mater. Chem.* **1999**, *9*, 2351; X. Shen, M. Belletête, G. Durocher, *Chem. Phys. Lett.* **1998**, *298*, 201.

[20] Y. Takashima, Y. Oizumi, K. Sakamoto, M. Miyauchi, S. Kamitori, A. Harada, *Macromolecules* **2004**, *37*, 3962; Y. Takashima, K. Sakamoto, Y. Oizumi, H. Yamaguchi, S. Kamitori, A. Harada, *J. Inclusion Phenom. Macrocyclic Chem.* **2006**, *56*, 45.

[21] M. van den Boogaard, G. Bonnet, P. van't Hof, Y. Wang, C. Brochon, P. van Hutten, A. Lapp, G. Hadziioannou, *Chem. Mater.* **2004**, *16*, 4383.

[22] K. Sakamoto, Y. Takashima, H. Yamaguchi, A. Harada, *J. Org. Chem.* **2007**, *72*, 459.

[23] E. J. F. Klotz, T. D. W. Claridge, H. L. Anderson, *J. Am. Chem. Soc.* **2006**, *128*, 15374.

[24] K. B. Lipkowitz, *Chem. Rev.* **1998**, *98*, 1829.

[25] M. L. Frampton, G. Sforazzini, S. Brovelli, G. Latini, E. Townsend, C. C. Williams, A. Charas, L. Zalewski, N. S. Kaka, M. Sirish, L. J. Parrott, J. S. Wilson, F. Cacialli, H. L. Anderson, *Adv. Funct. Mater.* **2008**, *18*, 3367; F. E. Oddy, S. Brovelli, M. T. Stone, E. J. F. Klotz, F. Cacialli, H. L. Anderson, *J. Mater. Chem.* **2009**, *19*, 2846.

[26] S. Brovelli, G. Latini, M. J. Frampton, S. O. Mcdonnell, F. E. Oddy, O. Fenwick, H. L. Anderson, F. Cacialli, *Nano Lett.* **2008**, *8*, 4546.

[27] R. Ahlrichs, M. Bar, M. Haser, H. Horn, C. Kolmel, *Chem. Phys. Lett.* **1989**, *162*, 165.

[28] W. L. Jorgensen, D. S. Maxwell, J. TiradoRives, *J. Am. Chem. Soc.* **1996**, *118*, 11225.

[29] C. I. Bayly, P. Cieplak, W. D. Cornell, P. A. Kollman, *J. Phys. Chem.* **1993**, *97*, 10269.

[30] G. Raos, A. Famulari, V. Marcon, *Chem. Phys. Lett.* **2003**, *379*, 364.

[31] J. C. Sancho-García, J. Cornil, *J. Chem. Theory Comput.* **2005**, *1*, 581.

[32] Gaussian 03, Revision C.02, M. J. Frisch, G. W. Trucks, H. B. Schlegel, G. E. Scuseria, M. A. Robb, J. R. Cheeseman, J. A. Montgomery, Jr., T. Vreven, K. N. Kudin, J. C. Burant, J. M. Millam, S. S. Iyengar, J. Tomasi, V. Barone, B. Mennucci, M. Cossi, G. Scalmani, N. Rega, G. A. Petersson, H. Nakatsuji, M. Hada, M. Ehara, K. Toyota, R. Fukuda, J. Hasegawa, M. Ishida, T. Nakajima, Y. Honda, O. Kitao, H. Nakai, M. Klene, X. Li, J. E. Knox, H. P. Hratchian, J. B. Cross, V. Bakken, C. Adamo, J. Jaramillo, R. Gomperts, R. E. Stratmann, O. Yazyev, A. J. Austin, R. Cammi, C. Pomelli, J. W. Ochterski, P. Y. Ayala, K. Morokuma, G. A. Voth, P. Salvador, J. J. Dannenberg, V. G. Zakrzewski, S. Dapprich, A. D. Daniels, M. C. Strain, O. Farkas, D. K. Malick, A. D. Rabuck, K. Raghavachari, J. B. Foresman, J. V. Ortiz, Q. Cui, A. G. Baboul, S. Clifford, J. Cioslowski, B. B. Stefanov, G. Liu, A. Liashenko, P. Piskorz, I. Komaromi, R. L. Martin, D. J. Fox, T. Keith, M. A. Al-Laham, C. Y. Peng, A. Nanayakkara, M. Challacombe, P. M. W. Gill, B. Johnson, W. Chen, M. W. Wong, C. Gonzalez, J. A. Pople, Gaussian, Inc., Wallingford CT, **2004**.

[33] W. Damm, A. Frontera, J. TiradoRives, W. L. Jorgensen, *J. Comput. Chem.* **1997**, *18*, 1955.

[34] Y. J. Zheng, R. L. Ornstein, *J. Am. Chem. Soc.* **1996**, *118*, 4175.

[35] B. Hess, C. Kutzner, D. van der Spoel, E. Lindahl, *J. Chem. Theory Comput.* **2008**, *4*, 435.

[36] B. Efron, R. Tibshirani, *Stat. Sci.* **1986**, *1*, 54.

[37] A. Grossfield, WHAM code available at: http://membrane.urmc.rochester.edu/Software/WHAM/WHAM.html

[38] A. Grossfield, D. M. Zuckerman, *Annu. Rep. Comput. Chem.* **2009**, *5*, 23.

[39] http://www.nist.gov/srm.

Received: December 7, 2009